UWB Indoor Delay Profile Model For Residential and Commercial Environments

S.S. Ghassemzadeh[1], L. J. Greenstein[2], A. Kavčić[3], T. Sveinsson[3], V. Tarokh[3]

***Abstract*— We present a statistical model for the delay profile of ultra-wideband channels in indoor environments. Two kinds of profiles are defined, namely the *multipath intensity profile* (MIP) and the *power delay profile* (PDP). The MIP is he delay profile at a point in space, while the PDP is a local spatial average. The model is based on 60,000 complex frequency response measurements from 20 commercial buildings and 20 residential homes, with the transmitter and receiver both in line-of-sight (LOS) and non-line-of-sight (NLS) of each other. Simulations using the PDP model show excellent statistical agreement with the measured data.**

***Index Terms*—Multipath Intensity Profile, multipath fading, Power Delay Profile, root mean square delay spread, UWB.**

I. Introduction

One proposed application of Ultra-Wideband (UWB) technology is to wireless personal area networks (WPAN), where the working environment would be inside residential and commercial buildings [1]. To characterize the radio channel of such environments over ultra-wide bandwidths, we conducted measurements in 20 single-family dwellings and 20 commercial locations, spanning a frequency range from 2 to 8 GHz. Large-scale propagation results from these measurements, specifically the path loss, are reported in a companion paper [2]. In this paper, we report on the features of small-scale propagation, specifically the delay profile.

Several statistical models for UWB channel behavior have been proposed, both in standards contributions (e.g., [3]) and in published papers [4]-[7]. Here, we build on the delay profile modeling approaches taken in [6] and [7], which were based on extensive measurements taken in homes and centered on 5 GHz. The differences in our new database are three-fold: (1) The measurement bandwidth is 6 GHz, rather than 1.25 GHz; (2) commercial buildings are measured in addition to homes; and (3) measurements are made at 25 spatial positions about each nominal location. The impact of the latter change is that it permits us to estimate the *power delay profile* (PDP), which is the local spatial average of the squared magnitude of the impulse response (normalized to have an area, over delay, of 1). The quantity modeled in [6] and [7] was the PDP at a single point, which we called the *multipath intensity profile (*MIP). Here, we model both the PDP and MIP, for both line-of-sight (LOS) and non-line-of-sight (NLS) paths. Our primary interest, however, is the PDP.

The paper is organized as follows: Section II describes our MIP modeling and its extension to PDP modeling. Section III describes the data collection and reduction. Section IV derives the models and quantifies their parameter values. In Section V, PDP models are presented, for both LOS and NLS paths, and are used to simulate a new database of complex frequency responses that well-matches the measured data.

This material is based upon research supported in part by the National Science Foundation under the grant No. CCR-0118701 and Alan T. Waterman award, grant No. CCR-0139398. Any opinions, findings and conclusions or recommendation expressed in this publication are those of the authors and do not necessary reflect the views of the National Science Foundation.

[1] S.S. Ghassemzadeh (saeedg@research.att.com, corresponding author) is with AT&T Labs-Research, Florham Park, NJ, USA.

[2] L.J. Greenstein is with WINLAB-Rutgers University, Piscataway, NJ, USA.

[3] A. Kavčić, T. Sveinsson and V. Tarokh are with the Division of Engineering and Applied Sciences, Harvard University, Cambridge MA, USA

II. Modeling Background

A. Definitions

Multipath channels are assumed to be linear and thus completely defined by their impulse responses. The time- and location-dependent impulse response for a given transmit-receive path can be written as

$$h(t,\tau,d)=\sum_{i=0}^{L\text{-}1}a_i(t,\tau,d)e^{j\phi_i(t,\tau,d)}\delta(\tau-\tau_i) \qquad (1)$$

where $a_i(t,\tau,d)$ and $\phi_i(t,\tau,d)$ are the amplitude and phase of the i^{th} multipath, arriving with excess time delay τ_i; d is the path length; and L is the number of resolvable multipaths.

The impulse responses of indoor UWB channels have been shown to be essentially time-invariant [5], which allows us to define the time-invariant multipath intensity profile for a given receiver position as

$$X(\tau)=\sum_{i=0}^{L\text{-}1}\tilde{P}_i\delta(\tau-\tau_i) \qquad (2)$$

where

$$\tilde{P}_i=\frac{|a_i|^2}{\sum_{i=0}^{L\text{-}1}|a_i|^2} \quad \text{and} \quad \sum_{i=0}^{L\text{-}1}\tilde{P}_i=1 \qquad (3)$$

Two key parameters used to characterize multipath are the

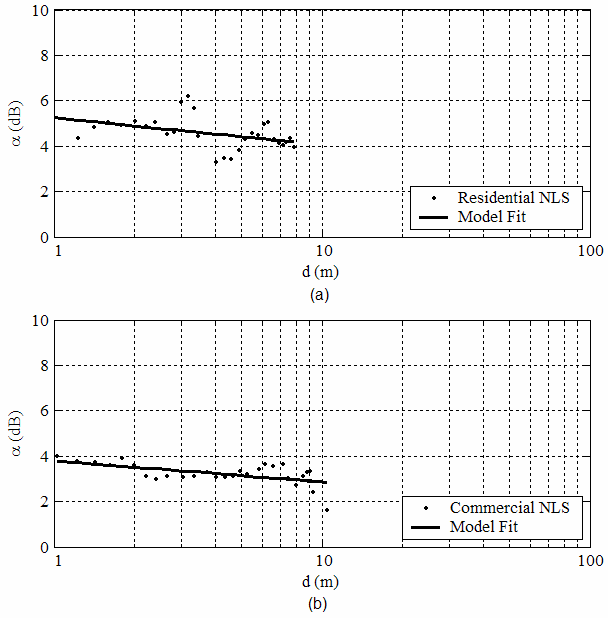

Fig. 1. Scatter plot of α vs. *d* for NLS paths: a) Residential, b) Commercial.

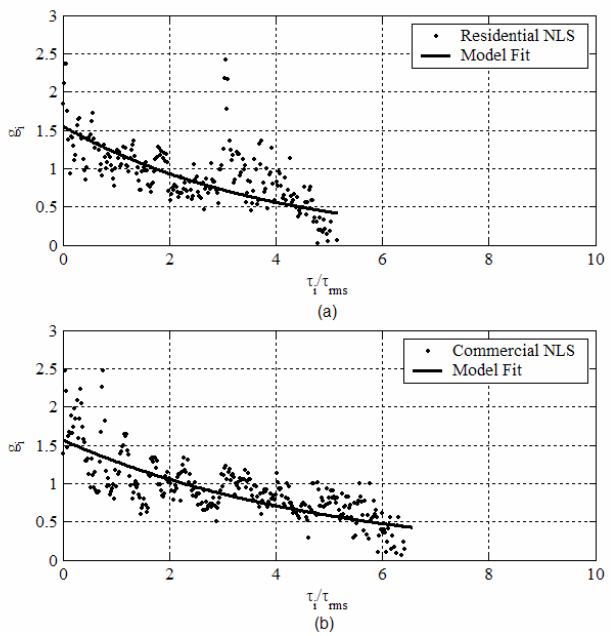

Fig. 2. Scatter plot of g_i vs. $\tau_i/\overline{\tau}_{\text{rms}}$ for NLS paths: a) Residential, b) Commercial.

mean excess delay, $\overline{\tau}$, and the rms delay spread, τ_{rms}, defined as

$$\overline{\tau} = \sum_{i=0}^{L-1} \tilde{P}_i \tau_i \text{ and } \tau_{\text{rms}} = \sqrt{\sum_{i=0}^{L-1} \tilde{P}_i \left(\tau_i - \overline{\tau}\right)^2} \tag{4}$$

Since the MIP, (2), is non-negative and integrates to 1, it has the properties of a probability distribution over the delay parameter, τ. Then, $\overline{\tau}$ and τ_{rms} can be viewed as the first moment and second central moment, respectively, of the MIP.

All of the above concerning the MIP applies equally to the PDP, with one difference: Each $|a_i|^2$ in (3) is replaced by its *local spatial average* value. In our measurements [2] and data reductions, 25 values of $|a_i|^2$ are obtained for each delay (indexed by i), corresponding to 25 spatial positions on a 20cm × 20 cm grid for each nominal location. Their numerical average is our estimate of the local spatial average of $|a_i|^2$. In what follows, the MIP and PDP are statistically modeled using the same process. For the MIP, only one point on the 25-point grid is used; in the PDP case, all are used.

B. Mathematical Form

Following [6] and [7], we treat the delay profile (MIP or PDP) as a decaying exponential over delay, multiplied by a lognormal process over delay. In dB form, the MIP is

$$P_i = \begin{cases} C & i = 0 \\ K - \alpha \cdot \tau_i / \overline{\tau}_{\text{rms}} + S_i & i > 0 \end{cases} \text{ for LOS}$$
$$P_i = K - \alpha \cdot \tau_i / \overline{\tau}_{\text{rms}} + S_i \quad i \geq 0 \text{ for NLS} \tag{5}$$

where P_i represents the dB values of $\tilde{P}_i$ in (3), C, K and α are constants defining the median profile, and $\overline{\tau}_{\text{rms}}$ is a normalizing parameter, so that α is dimensionless. (Our choice for $\overline{\tau}_{\text{rms}}$ is discussed later.) The deviations from this median are characterized by a zero-mean, normally distributed random process, S_i, with standard deviation σ_s. It can therefore be written as $S_i = y_i \sigma_s$, where y_i is a zero-mean, unit-variance normal random process on i. The main difference between LOS and NLS profiles is the strong term C at the lowest delay ($i = 0$) for LOS paths, corresponding to the direct ray from transmitter to receiver.

The model in [6] fits (5) to the data for each location; produces a common set of parameters for all locations in a given home; and then derives the distributions, over all homes, of the extracted parameters. The model in [7] provides a more in-depth characterization (as explained below) and achieves this by first pooling the data over all homes. In the present study, we apply the more detailed model of [7] to each residential (or commercial) building separately, and then characterize the variation over buildings of the extracted parameters.

III. Data Collection and Reduction

We used a network analyzer to measure complex frequency responses centered at 5 GHz, over a measurement bandwidth of 6 GHz. Data were collected in 20 homes and 20 commercial building sites, both on LOS and NLS paths. For each building type and path type, we chose about 30 receive locations, with transmitter-to-receiver separations ranging from 0.8 m to 10.5 m. For each location, we made 25 spatial measurements on a 20 cm x 20 cm horizontal grid. The total database thus consisted of about 60,000 complex frequency responses. For each measurement, we did the following:

– We removed the effects of hardware by using the stored calibration data. This included the antenna patterns.
– We performed a 1601-point inverse-Fourier transform, resulting in a complex impulse response with time delay ranging from 0 ns to 266 ns, with a bin size of 166.7 ps.
– We computed the magnitude-square of the complex impulse responses.
– We estimated the first multipath arrival and shifted the responses in time so that the first arrival time corresponds to 0 ns.
– For each location, we either used the data from the center of the grid only, to get the local MIP; or averaged the squared magnitudes over all 25 grid positions, to get the local PDP.
– Finally, we normalized the profile to achieve unit area with a noise floor of about 10 dB above the measurement equipment's average noise-floor.

The population of derived delay profiles is a 2×2 set, corresponding to two building types (residential and commercial) and two path types (LOS and NLS), with about 600 locations measured for each combination. In each of the four categories, we developed a statistical model for both the MIP and the PDP. The remainder of the paper describes these models and the comparisons among them.

IV. Model Fitting

A. Delay Spread Statistics

Using (4), we computed the delay spread statistics for individual profiles. Table I shows the statistics of τ_{rms} for residential and commercial buildings. For individual locations, we noticed that the delay spread found from either the MIP or its corresponding PDP was similar. In fitting data to (5), we use the same value for $\overline{\tau}_{\text{rms}}$ over all profiles within a common category of path type (LOS or NLS) and building type (residential or commercial). The value we use for each category is the average of the values in Table I for MIPs and PDPs.

B. Intra-Building Model Fitting

As a starting point, we fit (5) to all measured profiles. The result is a parameter set $\chi_1=\{C_{n,m}, \alpha_{n,m}, \sigma_{S,n,m}, d_{n,m}, \boldsymbol{y}_{n,m}\}$, where m is an index over locations within building n, and $d_{n,m}$ is the corresponding T-R separations. The vector $\boldsymbol{y}_{n,m}$ includes all y_i taken from building n and location m. We confirmed that $\boldsymbol{y}_n$ has a Gaussian distribution as reported earlier in [6] and [7]. We do not include the analysis of the constant K, since it is uniquely specified by the unit summation constraint.

Slope dependence on distance: The dependence between the slope $\{\alpha_m\}_n$ and T-R separation $\{d_m\}_n$ (over all locations m within the building n) is modeled as

$$\alpha_m(d_m) = \alpha_0 - \gamma \cdot \log_{10}(d_m) + \varepsilon \tag{6}$$

where α_0 and γ are constants and ε is a zero-mean Gaussian random variation with standard deviation σ_ε. The parameter α_0 is the average slope at the reference distance of 1 meter and γ captures the average slope decay with distance. Fig. 1 shows the scatter plot of α_m vs. d_m for NLS paths in typical residential and commercial settings. The result of fitting (6) to a single building indexed by n is the parameter set $\chi_2=\{\alpha_{0,n}, \gamma_n, \sigma_{\varepsilon,n}\}$.

Power dependence of the first return on distance: On LOS paths, the dependency between the power of the first multipath $\{C_m\}_n$ and the T-R separation $\{d_m\}_n$, is modeled as

$$C_m(d_m) = C_0 - \gamma_C \cdot \log_{10}(d_m) + \varepsilon_C\,, \tag{7}$$

where C_0 and γ_C are constants characterizing the average power of the first multipath at 1 meter, and its decay with distance, respectively. The random variation ε_C is zero-mean Gaussian, with standard deviation σ_C. Fitting (7) results in another set of parameters $\chi_3=\{C_{0,n}, \gamma_{C,n}, \sigma_{C,n}\}$.

Multipath correlation: We find the multipath correlation from the vector $\boldsymbol{y_n}$ using the same method as in [7]. We confirm that the correlation between multipaths arriving with a separation of k bins can be modeled by an exponentially decaying function,

$$\rho_y(k\Delta\tau) = \begin{cases} 1 & k = 0 \\ a \cdot e^{-b|k\Delta\tau/\overline{\tau}_{\text{rms}}|} & k > 0 \end{cases}, \tag{8}$$

where a and b are constants. The result is a set of correlation variables $\chi_4=\{a_n, b_n\}$ over buildings indexed by n.

Small-scale shadowing: Similar to [7], we decompose the random process y_i as

$$y_i = g_i \cdot x_i \tag{9}$$

where x_i is a stationary zero-mean, unit-variance Gaussian variation and g_i is a deterministic function of index i. From the vector $\boldsymbol{y}_n$, we analyzed g_i separately for each building and found it to be an exponential function of time delay,

Table I: Delay Characteristics For Residential And Commercial Buildings

		Residential			Commercial		
		$\overline{\tau}$ (ns)	$\overline{\tau}_{\text{rms}}$ (ns)	$\sigma_{\tau_{\text{rms}}}$ (ns)	$\overline{\tau}$ (ns)	$\overline{\tau}_{\text{rms}}$ (ns)	$\sigma_{\tau_{\text{rms}}}$ (ns)
MIP	LOS	2.22	3.72	1.67	4.24	5.95	1.59
	NLS	6.94	7.39	3.42	10.62	7.93	2.28
PDP	LOS	2.07	3.38	1.63	4.01	5.49	1.58
	NLS	6.91	7.31	3.47	10.37	8.15	2.45

Table II. STATISTICS OF MODEL PARAMETERS ACROSS RESIDENTIAL BUILDINGS

		LOS MIP		NLS MIP		LOS PDP		NLS PDP	
Set	Parameter	Mean	Std	Mean	Std	Mean	Std	Mean	Std
χ_2	α_0	2.35	0.86	3.97	1.15	3.51	1.49	5.29	2.02
	γ	0.45	1.06	1.62	1.69	1.28	1.72	2.30	2.88
	σ_ε	0.73	0.40	0.70	0.45	1.01	0.58	0.84	0.59
χ_3	C_0	-4.13	1.16	NA	NA	-4.07	1.23	NA	NA
	γ_C	1.39	1.55	NA	NA	1.35	1.71	NA	NA
	σ_C	1.12	0.25	NA	NA	0.84	0.22	NA	NA
χ_4	a	0.29	0.19	0.22	0.07	0.86	0.33	0.73	0.11
	b	0.20	0.10	0.21	0.06	0.19	0.08	0.15	0.04
χ_5	σ_0	2.54	0.24	2.44	0.43	2.16	0.30	1.77	0.29
	β	0.29	0.09	0.33	0.10	0.26	0.10	0.19	0.07
	σ_S	4.96	0.61	5.10	0.36	4.03	0.95	3.68	0.84

$$g_i = \sigma_0 \exp\left\{-\beta \frac{\tau_i}{\overline{\tau}_{\text{rms}}}\right\},\ \tau_i \geq 0\ . \tag{10}$$

Fig. 2 illustrates the scatter plot of g_i vs. $\tau/\overline{\tau}_{\text{rms}}$ for NLS paths in typical residential and commercial buildings. We estimated the parameters σ_0 and β for each building, and found $\sigma_{S,n}$ as the sample average of $\sigma_{S,n,m}$ (set χ_1) over different locations m for building n. The result is the parameter set $\chi_5=\{\sigma_{0,n},\beta_n,\sigma_{S,n}\}$.

C. Model Parameter Statistics

The sets χ_2, χ_3, χ_4 and χ_5 have model parameters for the full model, fitted to individual buildings. The statistics for the model parameters, over all buildings, are summarized in Tables II and III for residential and commercial buildings, respectively. We summarize our findings as follows.

Slope dependency on distance: From the set χ_2, we see that α_0 is higher for PDPs (faster decay) than for the MIPs; also that γ changes significantly between buildings and is inversely correlated with α_0. The cross-correlation coefficient between α_0 and γ is high (>0.54) for both MIPs and PDPs. We find α_0 to approximately follow a Gamma distribution over buildings, as does $\hat{\gamma} = \gamma + 2$ [1]. Fig. 3 shows the distribution of $\hat{\gamma}$ over buildings for NLS residential and commercial environments. The result is the same for LOS paths. We find σ_ε to have less variation between buildings than α_0 and γ, and to be uncorrelated with both of them.

Power dependency of first return on distance: We find C_0 and σ_C from χ_3, to be constant over buildings. The slope γ_C shows variation between buildings that can be modeled using a Gaussian distribution.

Multipath correlation: We found that the correlation between adjacent multipaths is generally small for MIPs. The mean of a (average correlation between two adjacent multipaths) is below 0.35 in all environments. Comparing the correlation for commercial and residential buildings, we find residential buildings to show significantly more correlation than commercial buildings. Also, the correlations are substantially higher for PDPs with the mean of a ranging from 0.54 to 0.86 over all environments.

Time delay dependence on model variations: We find the parameters σ_0, β and σ_S, to vary insignificantly between buildings. Also, σ_S is smaller for PDPs than for MIPs.

The key differences between the MIP and PDP models reside in the decay constant α, the lognormal standard deviation σ_S, and the correlations between paths. All these differences are explainable in terms of the averaging used to estimate the PDPs, which smooths both spatial variations and the effects of noise. Hereafter, we focus on the PDPs.

D. Key Parameters in a Simplified Model

A new PDP model can be constructed using the complete statistical characteristics of the channel. This approach is not chosen since it would result in high model complexity without sufficient increase in accuracy. Instead, we have chosen to limit the number of model parameters, focusing on capturing the key features of the PDPs.

From the results of the previous section and from model simulation experiments, we conclude that a simplified model

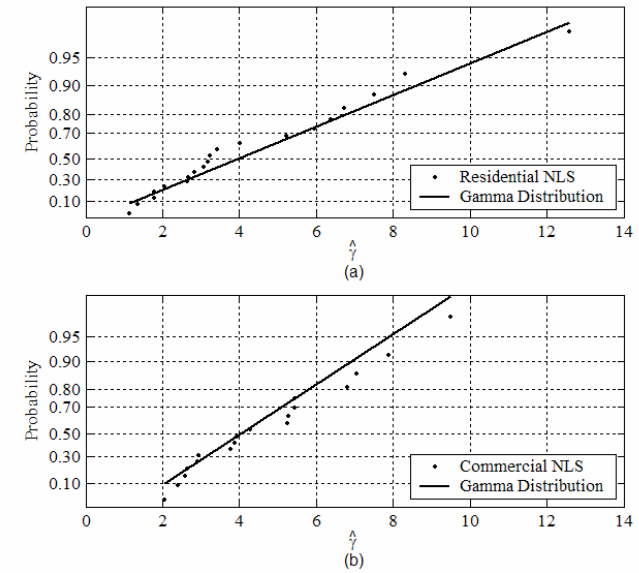

Fig 3. Distribution of $\hat{\gamma}$ for NLS paths: Residential (b) Commercial.

[1] We add 2 to γ to incorporate negative values of γ into the one-sided gamma distribution.

TABLE III. STATISTICS OF MODEL PARAMETERS ACROSS COMMERCIAL BUILDINGS

		LOS MIP		NLS MIP		LOS PDP		NLS PDP	
Set	Parameter	Mean	Std	Mean	Std	Mean	Std	Mean	Std
χ_2	α_0	1.99	0.76	3.33	1.15	2.98	1.46	5.13	1.56
	γ	-0.32	0.92	1.58	1.63	-0.22	1.76	2.67	2.09
	σ_ε	0.38	0.19	0.95	1.48	0.47	0.24	0.87	0.63
χ_3	C_0	-4.74	1.01	NA	NA	-4.68	0.93	NA	NA
	γ_C	2.45	2.06	NA	NA	2.38	1.97	NA	NA
	σ_C	1.16	0.27	NA	NA	0.88	0.20	NA	NA
χ_4	a	0.11	0.07	0.15	0.06	0.60	0.10	0.54	0.1
	b	0.16	0.06	0.20	0.08	0.21	0.08	0.12	0.05
χ_5	σ_0	2.55	0.25	2.25	0.39	2.10	0.18	1.76	0.34
	β	0.34	0.04	0.31	0.06	0.30	0.06	0.18	0.09
	σ_S	4.41	0.12	4.98	0.17	2.84	0.35	3.25	0.57

can be constructed using the parameters given in Tables II and III. The model components are as follows.

Parameters at the reference distance: We characterize the parameter α_0 in (6) as a constant with value fixed to its mean from Tables II and III. For LOS paths, we similarly define C_0 to be fixed.

Building dependency: We find γ and γ_C to vary between buildings. We characterize γ by the random variable $\gamma = \hat{\gamma} - 2$, where $\hat{\gamma}$ has a gamma probability distribution with density

$$p(\hat{\gamma} \mid A, B) = \frac{1}{B^A \Gamma(A)} \hat{\gamma}^{A-1} e^{-\frac{\hat{\gamma}}{B}} \tag{11}$$

and Γ(A) is the gamma function

$$\Gamma(A) = (A-1)! \tag{12}$$

The constants A and B are given in Table IV. For model simplicity, we fix γ_C to its mean value for each building type.

Distance dependency: We can capture the random effects of location (T-R separation) within a building on the slope α and first LOS path gain C. We do so via zero-mean Gaussian random variations ε and ε_C, with standard deviations σ_ε and σ_C, respectively. The parameters σ_ε and σ_C are fixed to their mean values for each building type.

Small-scale shadowing: For model simplicity, we set g_i at 1 over all i (i.e., y_i has the same variance over all i), eliminating parameters σ_0 and β. Also, we fix the correlation parameters a and b at their mean values, given in Tables II and III.

V. PDP MODEL AND SIMULATIONS

A. NLS Paths

Combining our findings, we construct the overall NLS PDP model from (5) to (10) as

$$P(\tau_i/\overline{\tau}_{\text{rms}}, d) = K - \alpha_0 \cdot \tau_i/\overline{\tau}_{\text{rms}} + \gamma \cdot \log_{10}(d) \cdot \tau_i/\overline{\tau}_{\text{rms}} + \varepsilon \cdot \tau_i/\overline{\tau}_{\text{rms}} + \sigma_S \cdot x_i \tag{13}$$

The model parameters are summarized in Tables IV. Again, the constant K, is found from the unit summation constraint on the PDP.

B. LOS Paths

From (5), we see that the LOS PDP model is based on the model for NLS environment for all multipaths except the first one. We characterize the first multipath by using (8). Then the complete model is given as

$$P(\tau_i/\overline{\tau}_{\text{rms}}, d) = \begin{cases} C_0 - \gamma_C \cdot \log_{10}(d) + \varepsilon_C & \text{for } \tau_i = 0 \\ K - \alpha_0 \cdot \tau_i/\overline{\tau}_{\text{rms}} & \\ +\gamma \cdot \log_{10}(d) \cdot \tau_i/\overline{\tau}_{\text{rms}} & \text{Otherwise} \\ +\varepsilon \cdot \tau_i/\overline{\tau}_{\text{rms}} + \sigma_S \cdot x_i & \end{cases} \tag{14}$$

where the model parameters are summarized Table IV. As for the NLS model, K is found such that the unit sum constraint is satisfied.

C. Simulations

We simulate the PDPs from (13) and (14) for the same number of buildings and set of distances as in our database. For simulation purposes, we first select either commercial or residential buildings, and then either NLS or LOS paths, and then choose the appropriate parameter values from Table IV. We then generate 20 realizations of γ (for 20 buildings). For each realization of γ, we generate 750 realizations of ε (30 T-R separations and 25 grid positions) and 750 realizations of ε_C if LOS paths are being simulated. For each realization of ε, we generate 1200 values of x_i (for multipaths with excess delay of 0 to 200ns), and construct a single PDP. Our aim is to calculate certain statistics from the simulated database of delay profiles and to compare them with those obtained from

TABLE IV. MODEL PARAMETERS VALUES.

	Residential		Commercial	
	LOS	NLS	LOS	NLS
α_0	3.51	5.29	2.98	5.13
A	3.69	2.72	1.53	5.58
B	0.89	1.58	1.31	0.84
σ_ε	1.01	0.84	0.47	0.87
C_0	–4.07	NA	–4.68	NA
γ_C	1.35	NA	2.38	NA
σ_C	0.84	NA	0.88	NA
a	0.86	0.73	0.60	0.54
b	0.26	0.15	0.21	0.12
σ_S	4.03	3.68	2.84	3.25
$\overline{\tau}_{rms}$	3.55	7.35	5.72	8.04

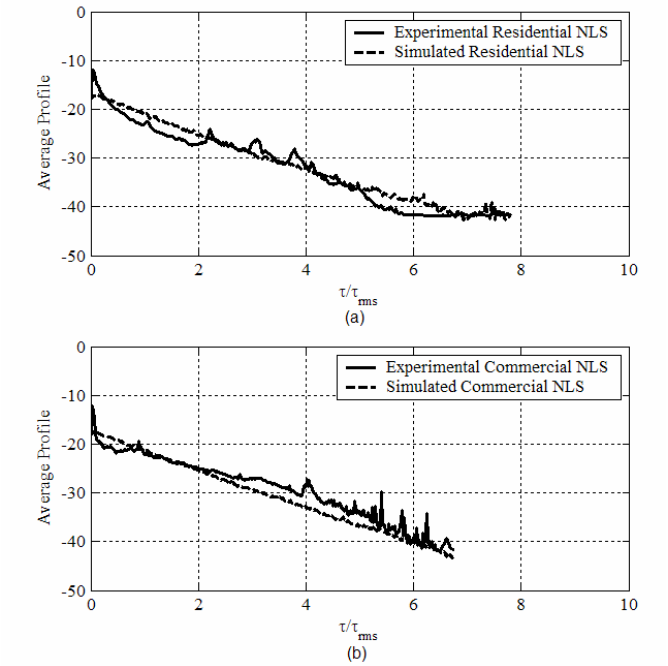

Figure 4. Average profiles for NLS paths: a) Residential, b) Commercial.

the measured database.

The average PDP for NLS paths in residential and commercial buildings are shown in Fig. 4. Probability distributions of the rms delay spread in residential buildings, for both LOS and NLS paths, are given in Fig. 5. In these comparisons of simulated and measured data, we find that the model performs very well, i.e., captures key statistical properties of the channel. Further comparisons are in progress.

VI. Conclusion

We have shown how ideas from two separate UWB multipath channel models, can be combined to capture detailed characteristics of the multipath channel and the statistical variability between buildings. Model simulations demonstrate good performance in capturing channel properties. Further data collection for both kinds of buildings would be helpful in confirming model stability. Meanwhile, testing of the model is continuing. Also, further data reductions, to characterize the spatial statistics at a location, would help to enrich the model.

Acknowledgement

The authors thank Dr. Alexander Hiamovich and Dr. Haim Grebel for use of their anechoic chamber at the New Jersey Institute of Technology; Mr. Chris Rice of AT&T Labs-Research, for valuable comments and suggestions on the hardware set-up; and lastly but not least, all the homeowners from AT&T Labs and Harvard University who graciously allowed us to invade their premises with our measurements.

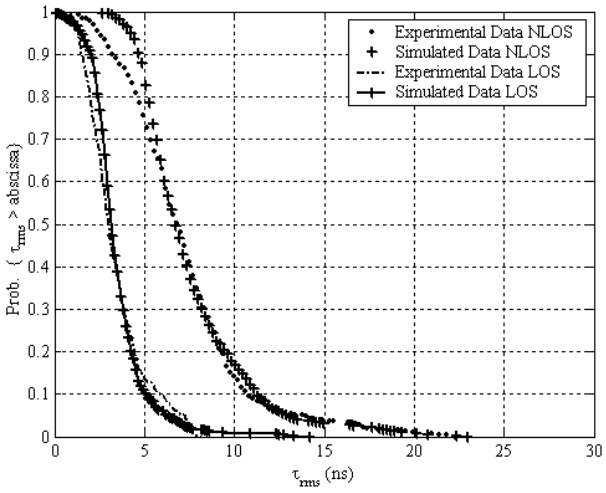

Figure 5. Commulative distributions of rms delay spread in residential buildings

References

[1] IEEE 802.15.3, IEEE standard for *wireless personal networks* (WPAN), URL: http://www.ieee802.org/15/pub/TG3a.html.

[2] S.S. Ghassemzadeh, L.J. Greenstein, A. Kavcic, T. Sveinsson, V. Tarokh, "Statistical path loss model for residential and commercial buildings", *Proceedings IEEE VTC Fall 2003*, October 2003.

[3] Channel-Modeling-Subcommittee-Report for IEEE-802.15.SG3a-URL:http://www.ieee802.org/15/pub/2003/Mar03/02490r1P802-15_SG3a-Channel-Modeling-Subcommittee-Report-Final.zip.

[4] D. Cassioli, M.Z. Win and A. Molisch, "The ultra-wide bandwidth indoor channel: from statistical model to simulations", *IEEE J. Sel. Areas Commun.*, Aug. 2002.

[5] S.S. Ghassemzadeh, et.al., "Measurement and modeling of an ultra-wideband indoor channel", *IEEE Trans. on Commun*., to appear.

[6] S.S. Ghassemzadeh, L.J. Greenstein, T. Sveinsson, and V. Tarokh, "A multipath intensity profile model for residential", *Proceedings IEEE WCNC-2003*, March 2003.

[7] ————, "An impulse response model for residential wireless channels", *Proceedings IEEE Globecom*, December 2003, to appear.